Supporting Information

Shao *et al.* 10.1073/pnas.0810388105

SI Materials and Methods

Animal Care

Male A/J, C57BL/6J, and C57BL/6J-Chr$^{A/J}$/NaJ mice were obtained from our breeding colonies. Mice were housed in ventilated racks and maintained at constant temperature (≈21 °C) and on a 12 h light/12 h dark cycle. Litters were weaned at 3 weeks of age. Mice had access to food and water ad libitum unless otherwise indicated. Laboratory Autoclavable Rodent Diet 5010 (LabDiet) was used for the breeding colonies.

Dissection. Following bleeding, mice were cervically dislocated. The mice were opened and all blood vessels leading to the liver were cut, starting anteriorly and working posteriorly, and allowed to bleed out. The liver was removed intact, weighed, and dissected for liver triglyceride determination. The same lobes of the liver were used for each experimental purpose whenever possible.

Biochemical Assays

Serology. At 21 weeks of age mice were fasted overnight (≈16–18 h), weighed, and anesthetized with an i.p. injection of 0.8-mg/g Avertin. Once anesthetized, nose-to-anus length and tail blood glucose measures (OneTouch Ultra, LifeSpan) were taken. With a heparinized microhematocrit capillary tube (Fisherbrand), ≈500 μL of blood was drawn from the retro-orbital sinus into a StatSpin blood separation tube and centrifuged for 4 min at ≈2000 × g in a bench-top minicentrifuge (Qualitron). Plasma was analyzed for cholesterol, glucose, and triglycerides by using commercially available reagents and standards (Pointe Scientific) in combination with a split-beam spectrophotometer (Genesys 5, Spectronic) following manufacturers procedures. Insulin was measured by using a mouse ultrasensitive insulin ELISA (Mercodia) in combination with a Wallac Victor^3 1420 Multilabel Counter (Perkin–Elmer).

Liver triglycerides. Liver samples were immediately frozen on dry ice and kept at −80 °C. To quantify the triglyceride content of the liver, between 100 to 200 mg of liver was saponified in an equal volume (μL) by weight (mg) of 3M KOH, 65% ethanol (1). After activation of the reaction at 70 °C for 1 h and incubation at room temperature for 24 h, the volume of each saponified liver was adjusted to 500 μL per 100-mg tissue used with 50 mM Tris (pH 7.5). Also, each sample was diluted 10-fold with 50 mM Tris (pH 7.5) before triglyceride determination. The liberated glycerol was measured against glycerol standards by using a commercially available triglyceride reagent (Pointe Scientific) in combination with a split-beam spectrophotometer (Genesys 5, Spectronic).

Homocysteine. Methods were described in ref. 2.

Bone Biology

Mice. Most CSSs were raised at Case Western Reserve University, except for several that were purchased from the Jackson Laboratory and raised at Mount Sinai School of Medicine. Mice were fed standard mouse chow (Purina Lab Chow 5001) and water ad libitum, and kept on a 12 h light:dark cycle.

Whole bone mechanical properties. Femurs from 112 day old A/J, C57BL/6J, and C57BL/6J-Chr$^{A/J}$/NaJ strains males and females at 4 months of age were loaded-to-failure in 4-point bending at 0.05 mm/s by using a servohydraulic materials test system (Instron) to assess whole bone mechanical properties (3). Load-deflection curves were analyzed for stiffness, maximum load, postyield deflection, and work-to-failure. These 4 monotonic properties fully describe the failure of mouse femurs (4). Stiffness was calculated as the slope of the initial portion of the load-deflection curve. Postyield deflection, a measure of bone ductility, was calculated as the deflection at failure minus the deflection at yield. Yield was defined as a 10% reduction of secant stiffness (load range normalized for deflection range) relative to the initial (tangent) stiffness. Work-to-failure was calculated as the area under the load-deflection curve. Femurs were tested at room temperature and kept moist with PBS during all tests. Means and standard deviations of each property were calculated for each strain.

Bone morphology. The morphological properties describing the size and shape of the femoral diaphysis were assessed with histological sections as described previously (3). Briefly, plastic-embedded femurs were sectioned transversely beginning immediately distal to the third trochanter. Morphological traits describing the amount of tissue (cortical area, cortical thickness) and the spatial distribution of tissue (periosteal diameter, polar moment of inertia) were quantified for 3 mid-diaphyseal cross-sections for each femur and the values averaged. Measuring both the amount and distribution of tissue is necessary because structures having the same cross-sectional area but different moments of inertia (e.g., a solid cylinder and a tube) will exhibit different mechanical behaviors in bending and torsion (5).

Composition. Ash content was quantified for the femurs subjected to mechanical testing (3). For each sample, the diaphysis was isolated, cleaned of soft tissue, and the hydrated weight, dried, and ashed weights were measured as described (3). Ash content was defined as the ash weight normalized for hydrated weight.

Congenic Panel Construction. Panels of congenic strains derived from C57BL/6J-Chr6$^{A/J}$/NaJ and C57BL/6J-Chr10$^{A/J}$/NaJ were constructed. For the CSS-6 congenic strains, F2 progeny of intercrosses between (C57BL/6J-Chr6$^{A/J}$/NaJ × C57BL/6J)F1 hybrids were genotyped with microsatellite markers to identify individuals that inherited recombinant A/J-derived chromosome 6. These F2 mice were backcrossed to C57BL/6J and offspring that were heterozygous for the selected region (identified by genotyping) were intercrossed to homozygose the A/J-derived segment. The congenic strains were then maintained with brother-sister matings. For CSS-10 congenic strains, (C57BL/6J-Chr10$^{A/J}$/NaJ × C57BL/6J)F1 hybrids were backcrossed to C57BL/6J and progeny were typed for microsatellite markers to identify individuals that inherited recombinant A/J-derived chromosome 10. These mice were then backcrossed to C57BL/J and offspring that were heterozygous for the recombinant chromosome were intercrossed to homozygose the A/J-derived segment. The congenic strains were then maintained with brother-sister matings.

Genotyping

DNA and PCR. For microsatellite markers (SSLPs), tail tissue was digested with proteinase K (Invitrogen) in 1× PCR buffer (Invitrogen) overnight at 55 °C. The enzyme was inactivated at 100 °C for 1 h before by using the DNA for genotyping. For single nucleotide polymorphisms (SNPs), DNA was isolated with standard methods (Qiagen DNeasy Kit). PCR reactions for SSLPs were performed in 1× PCR buffer, 2 mM MgCl2, 0.3 mM of each dNTP, 0.03 units of Taq polymerase/μL and 0.4–0.5 μM of forward and reverse primers in 25 μL total reaction volume. The reaction conditions were: 94 °C for 2 min, 94 °C for 1 min, 60 °C for 1 min, 72 °C for 1 min, repeat steps 2–4 34 times, 72 °C for

5 min, and 4 °C for 15 min. For SSLPs, PCR products were separated by using 6% polyacrylamide gel electrophoresis and visualized under UV light with ethidium bromide (Gel Doc 2000, Bio-Rad).

SSLPs and SNPs. Informative microsatellite (SSLP) markers were selected from NCBI (www.ncbi.nlm.nih.gov/genome/guide/mouse) and MGD (http://www.informatics.jax.org). All marker locations refer to NCBI Build 35 (http://www.ncbi.nlm.nih.gov/genome/guide/mouse). To refine the recombination breakpoints for the QTL critical regions of the intercross, additional microsatellite markers and SNPs were genotyped. SNP data were obtained from 4 sources: NCBI dbSNP (http://www.ncbi.nlm.nih.gov/SNP/mouseSNP.cgi), SNPview at GNF (http://snp.gnf.org/GNF10K) (6). The Inbred Laboratory Mouse Haplotype Map developed at the Broad Institute of Massachusetts Institute of Technology and Harvard (http://www.broad.mit.edu/personal/claire/MouseHapMap/Inbred.htm), and the Celera genome database (the original website is no longer available, but see ref. 7). For the CSS-6 intercross, the following SSLPs (*D6Mit#*) and SNPs were typed (m#, with alternative names and sequence coordinates (bp) given in parentheses from build 33 of the mouse genome–www.ncbi.nlm.nih.gov/genome/guide/mouse): m1 (3790155bp), m2 (*D6Mit138*; 4206900bp), m3 (23971862bp), m4 (*D6Mit159*; 29621200bp), m5 (36299590bp), m6 (*D6Mit223*; 45234635bp), m8 (47205158bp), m9 (*D6Mit274*; 48637500bp), m10 (51785906bp), m11 (54131745bp), m12 (54488587bp), m13 (*D6Mit384*; 55161700bp), m14 (73555817bp), m15 (*D6Mit188*; 75683000bp), m16 (*D6Mit391*; 85526100bp), m17 (87127482bp), m18 (*D6Mit284*; 92962700bp), m19 (*D6Mit36*; 104884300bp), m20 (107020358bp), m21 (*D6Mit287*; 112512600p), m22 (*D6Mit254*; 125974300bp), m23 (128402933p, m24 (137657411bp), m25 (*D6Mit159*; 139082100bp), m26 (*D6Mit15*; 146549700bp), m27 (146788578bp), and m28 (147857079bp). For constructing and analyzing the congenic strains, only the SSLPs listed in Fig. 3 were used.

For the CSS-10 intercross, the following SSLPs (*D10Mit#*) and SNPs were typed (m#, with alternative names and approximate sequence coordinates provided in parentheses): m1 (snp6355, rs3656355; 3.8Mb), m2 (snp9265, rs29375525; 7.2Mb), m3 (*D10Mit298*, 8.5Mb), m4 (*D10Mit167*; 18.1Mb), m5 (*D10Mit282*; 20.7Mb), m6 (*D10Mit106*; 24.1Mb), m7 (snp0569, rs13480569; 30.5Mb), m8 (snp2313, rs29318509; 43.1Mb), m9 (snp2938, rs29369275; 48.3Mb), m10 (snp1857, rs29359333; 57.9Mb), m11 (snp1818, rs29375724; 67.5Mb), m12 (snp6337, rs13480651; 73.8Mb), m13 (*D10Mit42;* 82.2Mb), m14 (*D10Mit230;* 89.8Mb), m15 (*D10Mit95;* 92.1Mb), m16 (*D10Mit70;* 103.6Mb), m17 (snp1162, rs29367042; 110.1Mb), m18 (*D10Mit180;* 117.7Mb), m19 (snpHmga2, rs13480792; 119.8Mb), m20 (snp6817, rs29331213; 125.2Mb), m21 (snp0830, rs13480830; 129.0Mb), m22 (*D10Mit189;* 18.1Mb), m23 (*D10Mit214;* 25.4Mb), m24 (snp0689, rs13480689, 87.0Mb), m25 (snp0690, rs13480690, 87.3Mb), m26 (snp0821, rs13480821, 127.0Mb), and m27 (snp0830, rs13480830, 129.0Mb). For constructing and analyzing the congenic strains, only the SSLPs listed in Fig. S2 were used.

SNP genotyping in the chromosome 6 intercross. SNPs were genotyped with the Sequenom MassArray 7K system and MALDI-TOF MS (matrix-assisted laser desorption/ionization time-of-flight mass spectrometry). For each marker, genotypes were scored independently with both the Sequenom software (version 3.3) and also with a second method developed by Joel Hirschhorn (personal communication). Generally, only markers in which 90% of the typed individuals had concordant, positive (not "no call") genotypes with both methods were used in the analysis. Among the concordant calls of usable markers, we tested whether the distribution of genotypes at each locus were consistent with Mendelian expectations for an intercross. Fit to expectations was evaluated with a χ^2 test at $P = 0.0016$, the Lander–Kruglyak threshold for an intercross (free model) (8). No markers on chromosome 6 deviated from the expected distributions.

1. Salmon DM, Flatt JP (1985) Effect of dietary fat content on the incidence of obesity among ad libitum fed mice. *Int J Obes* 9:443.
2. Ernest S, Hosack A, O'Brien WE, Rosenblatt DS, Nadeau JH (2005) Homocysteine levels in A/J and C57BL/6J mice: Genetic, diet, gender, and parental effects. *Physiol Genomics* 21:404–410.
3. Jepsen KJ, Pennington DE, Lee Y-L, Warman M, Nadeau J (2001) Bone brittleness varies with genetic background in A/J and C57BL/6J inbred mice. *J Bone Miner Res* 16:1854–1862.
4. Jepsen KJ, Akkus OJ, Majeska RJ, Nadeau JH (2003) Hierarchical relationship between bone traits and mechanical properties in inbred mice. *Mamm Genome* 14:97–104.
5. Meulen MCHvd, Jepsen KJ, Mikic B (2001) Understanding bone strength: Size isn't everything. *Bone* 29:101–104.
6. Wiltshire T, *et al.* (2003) Genome-wide single-nucleotide polymorphism analysis defines haplotype patterns in mouse. *Proc Natl Acad Sci USA* 100:3380–3385.
7. Cunningham F, *et al.* (2006) TranscriptSNPView: A genome-wide catalog of mouse coding variation. *Nat Genet* 38:853–853.
8. Lander E, Kruglyak L (1995) Genetic dissection of complex traits: Guidelines for interpreting and reporting linkage results. *Nat Genet* 11:241–247.

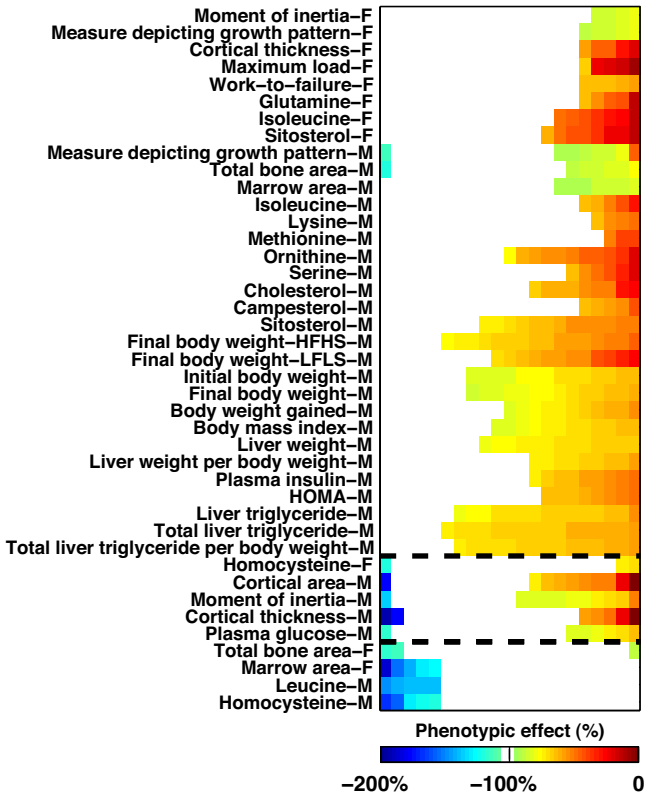

Fig. S1. Clustering of histograms of phenotypic effects. For each of the 41 multigenic traits in the panel, the CSS strains were ranked according to the normalized phenotypic shift and indicated with a colored box if the shift was significantly different from zero and by a blank box otherwise, with shifts toward A/J (*Right*) and away from A/J (*Left*). Traits were then clustered according to similarity of the overall pattern of normalized phenotypic differences. Cluster 1 (32 traits) with shifts strongly toward A/J; Cluster 2 (5 traits) with shifts both toward or away from A/J; and Cluster 3 (4 traits) with shifts away from A/J. F, female (all other traits were scored in males); HFHS, high-fat high-sucrose diet; LFLS, low-fat low-sucrose diet; HOMA, homeostasis model assessment.

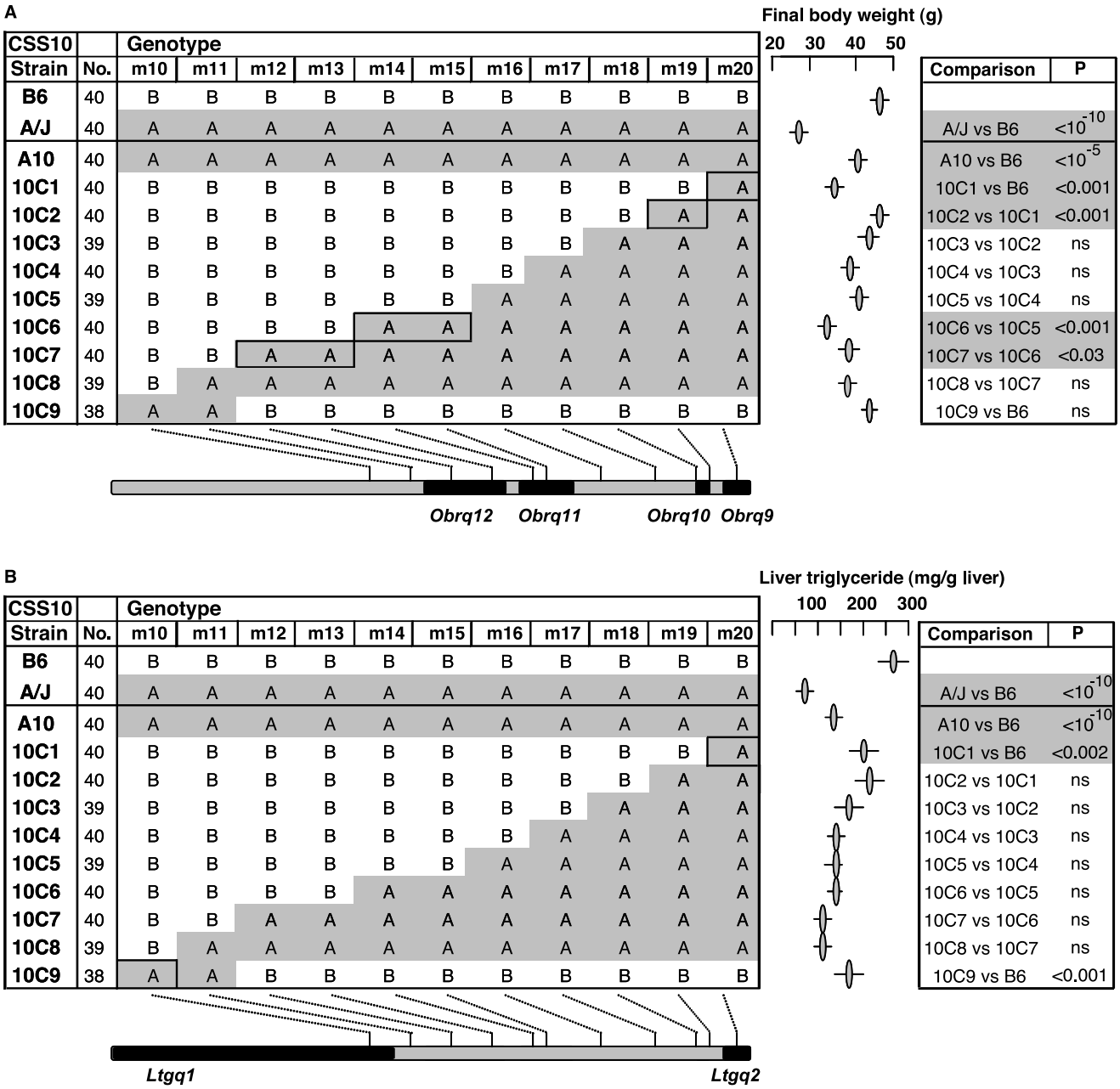

Fig. S2. Phenotypic effects and QTLs in congenic strains derived from CSS10. (*A*) Final body weight (FBW). (*B*) Liver triglycerides. Genetic markers (m), centromere (*Left*) and telomere (*Right*); ovals, mean trait value; whiskers on the ovals, SEM; and No., sample size. Pairwise comparisons between strains are indicated, by using 2-tailed *t* tests with significance levels (*P*) corrected for multiple hypothesis testing. The locations of A/J derived segments are indicated in gray, with the breakpoints of the congenic segments arbitrarily placed midway between the flanking markers, the locations of QTLs in the key congenic strains are indicated in boxes and correspond to the indicated segment (black) of the genetic map (*Bottom*), where the breakpoints for the most likely location for the QTLs are arbitrarily placed midway between the flanking markers. Connectors show the location of m in the congenic strains (*Top*, not to scale) and the genetic map (*Bottom*, at scale).

Table S1. Average and cumulative phenotypic effects for 90 traits in mouse and rat CSSs

Trait name	No. CSSs	Method, hi-low: Average effect, unsigned	Method, hi-low: Cumulative effect, %	Method, normalized units: Average effect, unsigned	Method, normalized units: Cumulative effect, %
		Mouse			
Blood					
Alanine	—	—	—	—	—
	—	—	—	—	—
Arginine	6	69.11	414.64	—	—
	4	51.81	207.25	—	—
Asparagine	—	—	—	—	—
	—	—	—	—	—
Campesterol	5	44.77	223.85	88.81	444.04
	—	—	—	—	—
Cholesterol	9	59.98	539.81	96.79	871.07
	—	—	——	—	
Citrulline	3	78.15	234.45	—	—
	—	—	—	—	—
Glutamic Acid	10	59.53	595.35	—	—
	14	70.81	991.33	—	—
Glutamine	3	41.26	123.79	—	—
	5	65.95	329.76	111.37	556.87
Glycine	—	—	—	—	—
	—	—	—	—	—
Histidine	—	—	—	—	—
	—	—	—	—	—
Homocysteine	5	34.36	171.82	81.16	405.82
	16	64.71	1035.38	—	—
	3	37.29	53.03	52.84	75.14
Isoleucine	5	65.51	327.57	99.73	498.64
	7	71.80	502.57	130.16	911.15
Leucine	5	42.48	212.39	83.25	416.24
	6	36.48	218.88	—	—
Lysine	4	83.00	331.98	91.48	365.93
	—	—	—	—	—
Methionine	3	73.07	219.22	112.66	337.98
	—	—	—	—	—
Ornithine	11	63.15	694.61	100.63	1106.93
	6	64.21	385.26	—	—
Phenylalanine	—	—	—	—	—
	—	—	—	—	—
Phosphoserine	—	—	—	—	—
	—	—	—	—	—
Proline	—	—	—	—	—
	—	—	—	—	—
Serine	6	61.45	368.70	112.64	675.85
	4	77.80	311.21	—	—
Sitosterol	13	63.95	831.37	77.09	1002.19
	8	52.77	422.18	127.11	1016.86
Taurine	—	—	—	—	—
	—	—	—	—	—
Threonine	—	—	—	—	—
	—	—	—	—	—
Tyrosine	—	—	—	—	—
	—	—	—	—	—
Valine	—	—	—	—	—
	—	—	—	—	—
Bone					
Ash content, %	—	—	—	—	—
	—	—	—	—	—
Cortical thickness, mm	7	32.78	80.66	148.38	365.12
	5	59.02	295.08	121.10	605.51
Cortical area, mm^2	10	30.71	221.07	108.35	780.08
	5	37.44	122.00	—	—
Moment of inertia, mm^4	11	30.46	253.44	51.46	428.18

Trait name	No. CSSs	Method, hi-low: Average effect, unsigned	Method, hi-low: Cumulative effect, %	Method, normalized units: Average effect, unsigned	Method, normalized units: Cumulative effect, %
	4	23.97	95.88	32.92	131.70
Measure depicting growth pattern, mm^2	8	26.58	174.41	35.07	230.09
	5	18.37	91.87	30.02	150.09
Marrow area, mm^2	7	21.88	153.13	24.35	170.46
	5	35.13	175.64	94.83	474.14
Maximum load, N	4	38.81	3.83	—	—
	5	43.10	215.49	145.60	727.99
Post-yield deflection, mm	—	—	—	—	—
	—	—	—	—	—
Stiffness, N/mm	3	74.43	223.30	—	—
	8	44.72	297.06	—	—
Total bone area, mm^2	7	23.16	103.24	32.81	146.29
	3	15.09	22.01	28.12	41.00
Work-to-failure, N·mm	—	—	—	—	—
	5	76.16	380.78	76.16	380.78
Metabolic					
Blood glucose, mg/dL	3	47.64	57.87	—	—
Body mass index, kg/m^2	12	46.28	555.34	55.09	661.05
Body weight gained, g	11	46.95	516.44	61.61	677.67
Final body weight, g	14	47.80	669.17	52.95	741.33
Final body weight, g-HFHS	16	58.00	927.97	75.36	1205.77
Final body weight, g- LFLS	12	59.53	714.41	95.52	1146.24
Homeostasis model assessment	8	60.15	481.22	83.65	669.16
Initial body weight, g	14	52.53	735.46	52.53	735.46
Liver triglycerides, mg/dL	15	52.69	790.34	63.05	945.80
Liver weight, g	13	34.70	451.12	56.65	736.50
Liver weight per body weight, %	9	28.14	253.26	64.50	580.48
Plasma cholesterol	7	29.93	162.13	46.87	253.92
Plasma glucose, mg/dL	—	—	—	—	—
Plasma insulin, μg/L	9	64.23	578.08	79.58	716.18
Plasma triglycerides, mg/dL	—	—	—	—	—
Total liver triglycerides, mg	16	48.52	776.30	69.28	1108.50
Total liver triglycerides per body weight, %	15	46.70	700.45	67.24	1008.61
		Rat			
Albumin, g/dL	—	—	—	—	—
	4	36.23	144.91	38.48	153.93
Alk phosphatase, units/L	4	42.77	47.77	186.27	208.04
	3	48.75	87.28	—	—
ALT, units/L	3	44.15	67.36	—	—
	—	—	—	—	—
Anion gap, mmol/L	10	34.03	4.46	—	—
	6	35.45	21.91	—	—
AST, units/L	—	—	—	—	—
	—	—	—	—	—
Bicarbonate, mmol/L	8	37.58	47.04	120.88	151.34
	—	—	—	—	—
Calcium, mg/dL	5	43.35	24.93	—	—
	—	—	—	—	—
Chloride, mmol/L	—	—	—	—	—
	—	—	—	—	—
Cholesterol, mg/dL	—	—	—	—	—
	7	28.53	102.94	38.12	137.55
Creatinine, mg/dL	6	38.89	150.00	—	—
	4	58.74	234.97	—	—
Globulin, g/dL	10	38.46	182.47	—	—
	11	38.92	231.48	—	—
Glucose, mg/dL	—	—	—	—	—
	—	—	—	—	—
Hematocrit, %	7	46.05	192.66	—	—
	10	57.29	572.93	—	—
Hemoglobin, g/dL	7	46.93	190.55	—	—

Trait name	No. CSSs	Method, hi-low: Average effect, unsigned	Method, hi-low: Cumulative effect, %	Method, normalized units: Average effect, unsigned	Method, normalized units: Cumulative effect, %
	9	59.34	534.03	—	—
Lymph abs, E3	4	53.73	214.92	—	—
	—	—	—	—	—
Mean corpuscular hemoglobin content, pg	5	38.69	40.93	97.34	102.99
	5	30.76	101.36	41.69	137.37
Mean corpuscular hemoglobin concentration, g/dL	—	—	—	—	—
	—	—	—	—	—
Mean corpuscular volume, fL	4	46.07	184.27	92.90	371.61
	8	29.03	184.84	38.06	242.29
Mono abs, E3	—	—	—	—	—
	4	84.75	339.01	—	—
Phosphorus, mg/dL	3	47.09	141.28	95.50	286.51
	—	—	—	—	—
Potassium, mmol/L	—	—	—	—	—
	3	74.28	222.84	—	—
Red blood cell count, E6/μL	6	41.14	85.10	89.48	185.09
	6	47.83	286.96	—	—
Segmented neutrophils, E3	—	—	—	—	—
	—	—	—	—	—
Sodium, mmol/L	4	45.97	93.92	—	—
	—	—	—	—	—
Total protein, g/dL	8	39.15	240.45	—	—
	7	44.55	311.82	55.99	391.90
Urea nitrogen, mg/dL	—	—	—	—	—
	—	—	—	—	—
White blood cell count, E3/μL	5	54.64	273.21	—	—
	—	—	—	—	—

Phenotypic effects are provided for surveys of blood, bone, and metabolic traits in surveys of the mouse and rat CSS panels. Two entries are made for many traits, with the upper value corresponding to data for males, and the lower to data for females. For multigenic traits, i.e., at least 3 CSSs differing significantly from the host strain, no. CSS denotes the number of CSSs with significant effects after correction for multiple hypothesis testing. Two methods were used to assess average and cumulative phenotypic effects: normalized units and hi-low (see *Materials and Methods*). The former was used for the analysis presented in the main text and the latter was an alternative analytical method. The 2 methods gave highly concordant results. For each trait, the average (unsigned) effect is listed together with the cumulative phenotypic effects as a percentage of the difference between the host and donor strains. Results for the mouse have been deposited in the Mouse Phenome Database (www.jax.org/phenome).

Table S2. Results of test for additivity for the 41 traits that differ significantly between the C57BL/6J and A/J parental strains

Trait	Males	Females
CtAr	0.001635	23.42162
Jo	0.000199	23.36347
Jo/A	0.01149	38.6366
Tar	3.691569	1.523602
Mar	2.295247	5.34E-06
Ash	5.914811	65.31262
CortThick	0.949231	0.205332
Stiffness	0.616087	0.658509
MaxLd	14.32031	24.87869
PYD	72.26927	0.72576
Work	29.01291	0.519314
HCY	1.51E-28	32.6465
Phosphoserine	52.32946	39.77178
Taurine	28.65821	3.643139
Threonine	75.79999	47.74512
Serine	1.241689	0.919207
Asparagine	25.41273	23.43951
Glutamic acid	2.945649	4.36E-05
Glutamine	11.36827	0.40516
Proline	54.3612	26.13294
Glycine	28.32468	36.09395
Alanine	62.62397	8.464281
Citrulline	0.771831	44.46014
Valine	7.353237	85.6979
Methionine	26.65632	11.09739
Isoleucine	1.098249	0.003235
Leucine	0.053641	3.329307
Tyrosine	48.72865	31.38236
Phenylalanine	82.06938	39.54256
Ornithine	0.0005	0.105953
Lysine	4.4715	5.408058
Histidine	56.95053	25.18625
Arginine	0.004222	7.873186
Cholesterol	0.003997	38.70646
Campesterol	30.84935	36.27179
Sitosterol	3.45E-05	0.802763
I-BW	8.08E-05	NA
F-BW	0.00013	NA
BWG	0.051785	NA
BMI	0.002512	NA
LWt	0.208115	NA
LWperBW	15.79331	NA
B-GLU	16.92633	NA
P-GLU	12.17238	NA
P-INS	0.003047	NA
HOMA	0.005745	NA
P-CHOL	12.38178	NA
P-TRIG	5.752733	NA
L-TRIG	5.05E-05	NA
TL-TRIG	0.039035	NA
TL-TRIGPerBW	0.050108	NA
HFHS_FBW	1.04E-06	NA
LFLS_FBW	0.000358	NA

Results are tabulated separately for females and males after Bonferroni correction for multiple hypothesis testing. $P < 0.05$ indicates a statistically significant departure from the additive model.

Other Supporting Information Files

SI Appendix

SI Appendix

Phenotypic effect

Two different estimations of phenotypic effect were used. First, we estimated phenotypic effects as a function of the phenotypic difference between the CSS Donor and Host strains:

$$ES_i = 100*[CSS_i - Host]/[Donor - Host]$$

Second, we noted that the range of mean trait values among the strains in a CSS panel as well as the two parental strains defines the total phenotypic variance, which includes both the genetic and error variance. We therefore computed the phenotypic effect (ES_i) for the *i*th CSS as:

$$ES_i = 100*[CSS_i - Host]/[Hi - Low]$$

where Host is the phenotypic value of the strain that was used as the background onto which chromosomes from the donor strain were substituted, Hi is the highest mean phenotypic value among the progenitor strains and the CSS panel, and Low is the strain with the lowest mean phenotypic value.

Standard error of measurement (SEM) for the cumulative effect

Next we consider methods for estimating SEM of individual and cumulative effects variable *w* from other variables.

In general, if $w = f(x, y, \ldots)$, then the SEM of *w*, $S(w)$ is $g(x, y, \ldots)$. For simplicity, we only use two variables in the following equation:

$$S(w) = \sqrt{\left(\frac{\partial w}{\partial x}\cdot S(x)\right)^2 + \left(\frac{\partial w}{\partial y}\cdot S(y)\right)^2 + 2r_{xy}\left(\frac{\partial w}{\partial x}\cdot S(x)\right)\cdot\left(\frac{\partial w}{\partial y}\cdot S(y)\right)}$$

If the correlation coefficient of relationship between two variables *x* and *y*, r_{xy}, is 0, then the estimation of *S(w)* can be simplified as the following:

$$S(w) = \sqrt{\left(\frac{\partial w}{\partial x} \cdot S(x)\right)^2 + \left(\frac{\partial w}{\partial y} \cdot S(y)\right)^2}$$

We used this equation to calculate the SEM for the individual and cumulative phenotypic effects. Let *X* be the mean trait value of CSS_i, *Y* be the trait value for C57BL/6J, *R* the value for A/J, *P* the value for Hi, and *Q* the value for Low. Let S_i be the standard error of the phenotypic effect of CSS_i, w_i be the effect of *i*th CSS compared to C57BL/6J. The following calculations were made:

- For each trait, estimate phenotypic effect in their measured units for CSS_i, the cumulative phenotypic effect, the SEM of the phenotypic effect, and finally the SEM of cumulative effect:

  The phenotypic effect for CSS_i is $w_i = (X_i - Y)/(R-Y)$.

  The cumulative phenotypic effect is $\sum w_i = \sum (X_i - Y)/(R-Y)$.

  The SEM for the phenotypic effect of CSS_i is

  $$S_{w_i}^2 = C_0 S_i^2 + C_1 (X_i - R)^2 + C_2 (X_i - Y)^2$$

  where $C_0 = 1/(R-Y)^2$, $C_1 = C_0^2 S_Y^2$, and $C_2 = C_0^2 \cdot S_R^2$.

  The SEM for the cumulative phenotypic effect is $S_{cum}^2 = \sum S_{w_i}^2$.

  Let *W* be the difference between the cumulative phenotypic effect and that of parental effect:

  $$W = \sum_i (X_i - Y)/(R-Y) - 100\%$$

  The SEM of *W* is the same as that for the cumulative phenotypic effect.

- For each trait, estimate the phenotypic effect for CSS_i with the Hi-Low method. In general, SEM of the cumulative effect is estimated as follows:

  after the derivative,

  $$S_{w_i}^2 = \frac{1}{(P-Q)^2}(S_{X_i}^2 + S_Y^2) + \frac{(X_i - Y)^2}{(P-Q)^4}(S_P^2 + S_Q^2)$$

  where P, Q, X and Y are defined above.

  Let $C_1 = 1/(P-Q)^2$, $C_0 = C_1 \cdot S_Y^2$, and $C_2 = C_1^2 \cdot (S_P^2 + S_Q^2)$

  Then for each CSS effect, SEM square is:

  $$S_{w_i}^2 = C_0 + C_1 \cdot S_i^2 + C_2 \cdot (X_i - Y)^2 = C_0 + C_1 \cdot S_i^2 + C_2 \cdot (X_i - Y)^2 .$$

  The cumulative effect is estimated as follows:

  $$S_{cum}^2 = \sum S_{w_i}^2 .$$

  For the difference between cumulative effect and 100%, S is the same as S^2_{cum}.

  But there are exceptions where the SEM of the cumulative effect is estimated differently.

  a. When CSS_i is Hi or Low, the estimation of SEM is as follows:

  $$W_i = \frac{X_i - Y}{X_i - Q} = 1 + \frac{Q - Y}{X_i - Q}$$

  $$S_{w_i}^2 = C_0 + C_1^2 \cdot [(X_i - Q)^2 \cdot S_P^2 + (X_i - P)^2 \cdot S_Q^2]$$

  where *i* is the *i*th CSS with highest or lowest mean trait value, C_0, and C_1 are defined as before.

  b. When C57BL/6J or A/J is Hi or Low, the estimation of SEM is as follows:

  without loss of generality, assume that B6 is Hi, then P = Y

$$W_i = \frac{X_i - Y}{Y - Q}$$

$$S_{w_i}^2 = C_1 \cdot S_{X_i}^2 + C_1^2 \cdot [(X_i - Q)^2 \cdot S_P^2 + (X_i - P)^2 \cdot S_Q^2]$$

When C57BL/6J is Hi or Low and one of the CSSs is Low or Hi, it is straightforward that ES = 100% and the standard error is estimated as zero.

Clustering of QTL direction effects

For any given trait, assume that N bins, the maximum trait value is Max, the minimum trait value is Min and Interval is (Max-Min)/2N. Given any trait value x, the estimated bin number, B, that x will be assigned to is:

B= [((x – Min-Interval) * N /(Max - Min))],

where [x] represents the nearest integer to x, and the residual is

res = (x – Min-Interval) * N/(Max-Min) – B

The number of trait that falls into B is updated as following:

Hist(B) = Hist(B)+ (1 –abs(res/(Max-Min)));

Hist(B+sign(res)) = Hist(B+sign(res)) + abs(res/(Max-Min))

such that the residual contributes to the closer bin of the two adjacent bins. A Gaussian filter was then used to smooth the resulting histogram for each trait. A vector was constructed to represent each trait, each of which consists of the number of peaks that appear before and after r equals 0 (see above) and their corresponding locations.

K-means was used to cluster the histograms of all 41 traits with CSS entries that differed significantly from C57BL/6J. The maximum cluster number was set to four, with squared Euclidean distance as the metric and a maximum iteration of 100. Empty clusters were not considered in subsequent analyses.